Angular Distributions for the Complete Photofragmentation of the Li Atom

J. Colgan and M. S. Pindzola

Angular distributions for the complete photofragmentation of the Li atom

J. Colgan

Theoretical Division, Los Alamos National Laboratory, Los Alamos, NM 87545

M. S. Pindzola

Department of Physics, Auburn University, Auburn, AL 36832

We explore the complete break-up of the Li atom after absorption of a single photon, the purest example of the so-called four-body Coulomb problem. The resulting strongly-correlated three-electron continuum is investigated by calculating the angular distributions of the ionized electrons using advanced close-coupling techniques. We find that the distributions are dominated by the Coulomb interactions between the electrons, that multiple break-up processes can be identified, and that the complex dynamics of the fragmentation process are evident for most scattering geometries.

PACS numbers:

The quantal four-body Coulomb problem, that of three charged particles moving in the field of a fourth charged body, presents a major challenge to our ability to accurately describe complex scattering problems beyond many-body perturbation theory [1]. It is only recently that the cleanest three-body Coulomb problems, manifested in the double photoionization of He or the electron-impact ionization of H, have been solved to suitable accuracy. It is now the case that experiment and theory are generally in excellent agreement for both of these scattering problems [2–6], and significant progress has also been made in examining similar scattering problems from small molecules [7–11].

The four-body Coulomb problem can be found in a multiple photoionization process or in an electron-impact ionization process. The latter has recently been the subject of intensive experimental and theoretical scrutiny in studies of the electron-impact double ionization of He [12–15]. The triple photoionization of Li (although strictly a five-body system if one includes consideration of the photon) has so far not been subject to experimental study in terms of capturing the ionized electrons after photon absorption, although a related measurement has been recently reported that captured core-valence-valence electrons after triple photoionization of Ne [16]. Another recent study examined triple photoionization from Li-like ions [17]. The sparse experimental work on Li is no doubt in part due to the small nature of the Li triple photoionization total cross section [18, 19], which peaks at around 10 barns, three orders of magnitude smaller than typical double photoionization total cross sections. However, a complete characterization of the triple photoionization of Li is of fundamental importance, since it represents the *cleanest* four-body Coulomb problem as the one-photon absorption leads to continuum electrons with a well defined total $\mathcal{LS}$ symmetry.

There have been few previous studies of the complete break-up of the Li atom by a single photon absorption. Some early studies explored the selection rules for three continuum electrons [20, 21], and used approximate 6C wavefunctions to provide some qualitative examples. The most relevant selection rule discussed for Li photofragmentation was that the pentuple differential cross section must be zero if all electrons are emitted in a plane perpendicular to the polarization axis, for states with $M = 0$ and odd parity. More recent studies used a quasi-classical approach to study Li triple photoionization near the triple ionization threshold [22, 23]. The latter study predicted that the ionized electrons resulting from triple ionization of ground-state Li should escape via a **T**-shape break-up pattern, due to the stability properties of the classical fixed point for multiple threshold fragmentation. Other break-up patterns for multiple electron ionization were also predicted, and one of these (the "triangle" break-up) was recently confirmed experimentally for electron-impact double ionization of He near threshold [13]. The time-dependent close-coupling (TDCC) method has also been used to compute total cross sections for Li and Be [24, 25], as well as energy differential cross sections for Li [26].

In this letter, we extend the TDCC approach to examine angular distributions of the outgoing electrons after triple photoionization of Li. A previous implementation of a similar three-electron approach to electron-impact double ionization of He was recently published [15], but this marks the first quantum-mechanical approach to the angular distributions corresponding to the triple photoionization of Li. We perform our calculations at photon energies away from threshold, and close to the peak of the total triple photoionization cross section, maximizing the magnitude of the resulting angular distributions. Although we find some break-up geometries which resemble the **T**-shape break-up pattern predicted near threshold [23], in general we find that the three-electron break-up is a complicated process and that many fragmentation geometries are possible.

We begin with a fully correlated wavefunction for the initial state of Li, which is obtained by solution of the time-dependent Schrödinger equation in imaginary time [24, 25], resulting in a ground-state energy E_0, which is within 2%

of the exact value of -203.4 eV. The fully correlated wavefunction for the final state of Li is obtained by solution of the time-dependent Schrödinger equation in real time with $P(r_1, r_2, r_3, t = 0) = 0$.

By expansion of the electronic wavefunctions in terms of products of radial wavefunctions and coupled spherical harmonics, the time-dependent Schrödinger equation can be reduced to time-dependent close-coupled equations [24, 25]. For example, the set of coupled equations which must be solved for the real-time propagation is given by

$$i\frac{\partial P^{\mathcal{L}}_{l_1 l_2 L l_3}(r_1, r_2, r_3, t)}{\partial t} \tag{1}$$

$$= T_{l_1 l_2 l_3}(r_1, r_2, r_3) P^{\mathcal{L}}_{l_1 l_2 L l_3}(r_1, r_2, r_3, t)$$

$$+ \sum_{l_1', l_2', L', l_3'} \sum_{i<j}^{3} V^{\mathcal{L}}_{l_1 l_2 L l_3, l_1' l_2' L' l_3'}(r_i, r_j) P^{\mathcal{L}}_{l_1' l_2' L' l_3'}(r_1, r_2, r_3, t)$$

$$+ \sum_{l_1', l_2', L', l_3'} \sum_{i}^{3} W^{\mathcal{L}\mathcal{L}'}_{l_1 l_2 L l_3, l_1' l_2' L' l_3'}(r_i, t) \bar{P}^{\mathcal{L}'}_{l_1' l_2' L' l_3'}(r_1, r_2, r_3) e^{-iE_0 t}$$

for $\mathcal{L} = 1$ and $\mathcal{L}' = 0$, and where $\bar{P}$ is the initial state radial wavefunction. The forms of the kinetic and nuclear energy operator, T, the electron-electron interaction operator, V, and the photon-electron operator, W, are given in previous work [25].

After time propagation of Eq. (1), the final state radial wavefunctions, $P^{\mathcal{L}}_{l_1 l_2 L l_3}(r_1, r_2, r_3, t)$, are projected onto fully antisymmetric products of one-electron spin orbitals to obtain final state momentum space wavefunctions [25]. For the triple photoionization of Li, with $\mathcal{L} = 1$ and $\mathcal{S} = \frac{1}{2}$, one may then define total and energy differential cross sections, as previously discussed [25, 26]. To compute angular distributions for the three outgoing electrons, we define a pentuple energy and angle differential cross section by:

$$\frac{d^5\sigma}{dE_2 dE_3 d\Omega_1 d\Omega_2 d\Omega_3} = \frac{1}{k_1 k_2 k_3 \sqrt{k_1^2 + k_2^2}} \frac{\omega}{I} \frac{\partial}{\partial t}$$

$$\times \int_0^\infty dk_1 \int_0^\infty dk_2 \int_0^\infty dk_3 \delta\left(\alpha - \tan^{-1}(\frac{k_2}{k_1})\right)$$

$$\times \delta\left(\beta - \tan^{-1}(\frac{k_3}{\sqrt{k_1^2 + k_1^2}})\right)$$

$$\times \sum_S \frac{1}{6} \sum_{ijk}^6 |\sum_{l_1, l_2, l_3, L} (-i)^{l_1 + l_2 + l_3} e^{i(\delta_{l_1}(k_i) + \delta_{l_2}(k_j) + \delta_{l_3}(k_k))}$$

$$\times P^{\mathcal{L}\mathcal{S}}_{l_1 \frac{1}{2} l_2 \frac{1}{2} L S l_3 \frac{1}{2}}(k_i, k_j, k_k, t) \mathcal{Y}_{l_1 l_2 L l_3}(\Omega_i, \Omega_j, \Omega_k)|^2 , \tag{2}$$

where ω is the field frequency, I is the field intensity, α and β are angles in the three-dimensional hyperspherical plane, δ_l is a Coulomb phase shift, and $\mathcal{Y}$ is a coupled product of three spherical harmonics. The integrals over linear momenta, k_i, are restricted so that the total energy $E_0 + \omega = \frac{k_1^2}{2} + \frac{k_2^2}{2} + \frac{k_3^2}{2}$ is conserved.

In the calculations discussed here, a box of $(192)^3$ points was used, with a mesh spacing of $\Delta r = 0.1$ a.u. Although this is a relatively small mesh size, we found that calculations which doubled the radial mesh (i.e. using $(384)^3$ points) made little difference to the angular distributions at a photon energy of 300 eV. At 230 eV the angular distributions are more sensitive to the mesh size, and at lower photon energies, significantly larger meshes are expected to be required for convergence. We also found that convergence with respect to the number of coupled channels included in the expansions of Eq. (1) was slow. The calculations presented here included all channels up to and including $l = 6$, which results in 270 coupled channels for the final $^2\mathcal{P}$ state and 144 determinental states used in the projections. Such calculations required the efficient use of massively parallel supercomputing resources. Calculations which included coupled channels up to, say, $l = 3$ resulted in angular distributions which were quite different to those presented below. At larger photon energies, it is likely that even more coupled channels will be required for convergence.

There have been no measurements made of the electron angular distributions for Li triple photoionization, and no previous quantitative calculations are available with which to compare. We can compare with the qualitative results of Maulbetsch and Briggs [20] and we confirm their proposed selection rule, i.e. that there is zero cross section for geometries where all three electrons are ejected perpendicular to the polarization axis. Incidentally, we also find a similar cosine-squared angular distribution for the third electron, when the remaining two electrons are fixed back-to-back and perpendicular to the polarization axis, as found in Figure 1(a) of [20], although our calculations were
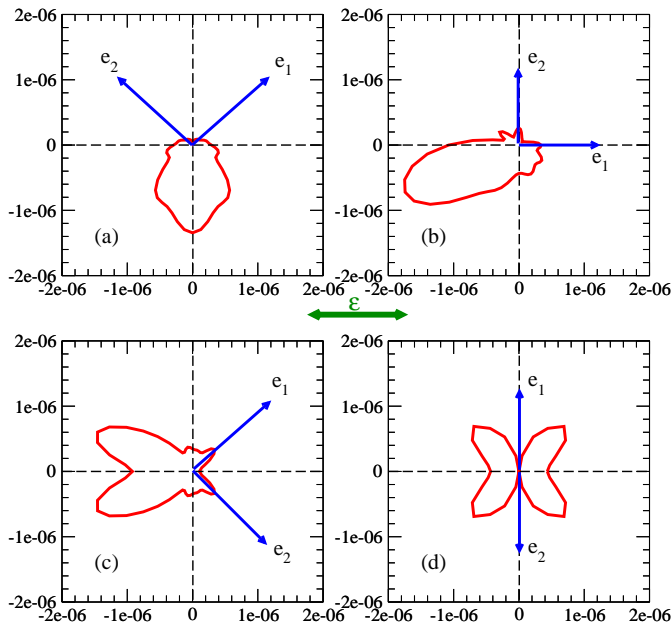
FIG. 1: (Color online) Pentuple differential cross sections for triple photoionization of Li at a photon energy of 300 eV and for $E_1 = E_2 = E_3 = 33$ eV. Results are presented as a function of θ_3 for fixed values of θ_1 and θ_2. (a): $\theta_1 = 45°$, $\theta_2 = 135°$; (b): $\theta_1 = 0°$, $\theta_2 = 90°$; (c): $\theta_1 = 45°$, $\theta_2 = 315°$; (d): $\theta_1 = 90°$, $\theta_2 = 270°$. All cross sections are in units of b/(sr^3 eV^2).

carried out at much larger photon energies than the threshold studies performed by Maulbetsch and Briggs. This is found in our calculations for all equal energy sharing cases.

In Figure 1 we present pentuple differential cross sections for the triple photoionization of Li at a photon energy of 300 eV. Angular distributions are presented for equal energy sharing ($E_1 = E_2 = E_3 = 33$ eV), in the coplanar geometry ($\phi_i = 0$ for $i = 1 - 3$) for fixed θ_1 and θ_2 values, and as a function of the third θ_3 angle. In the polar plots of Figure 1, the polarization direction is horizontal as indicated, where $\theta_i = 0°$ along this direction.

A major finding of the earlier studies of photofragmentation of Li in the threshold region [23] was that, from the Li ground-state, the fragmentation would proceed primarily in a **T**-shape, i.e. two electrons ejected back-to-back, with the third electron perpendicular to this axis. In Figure 1 we explore such possible break-up patterns. In Figure 1(a), the first two electrons are fixed at $45°$ and $135°$ as indicated. We find that the third electron is ejected predominantly at an angle of $270°$. This is not unexpected, as this is the angle at which Coulomb repulsion pushes the third electron furthest away from the other two electrons. However, this break-up pattern is more indicative of the "triangle" ($\triangle$) geometry found previously for three-electron break-up in double ionization of He by electron-impact [13] (or predicted for photofragmentation of Li from an excited $1s2s^2$ state [23]). In Figure 1(c) we examine a similar break-up geometry: $\theta_1 = 45°$ and $\theta_2 = 315°$. We might at first expect the same angular distribution pattern as found in Figure 1(a), since the angle between electrons 1 and 2 are the same. However, we find that the angular distribution of the third electron is somewhat more complex (although still predominantly along the direction maximizing the distance between the outgoing electrons). The difference between Figure 1(a) and (c) is due to the polarization direction, which appears to significantly influence the angular distributions. In Figure 1(c) we find that the third electron is less likely to travel along the polarization direction.

Although Figures 1(a) and (c) indicate that a triangle break-up geometry is more favored, when we examine other angular distributions this is not necessarily the case. Figure 1(b) shows the θ_3 angular distribution for $\theta_1 = 0°$ and $\theta_2 = 90°$. In this case we find that the third electron is ejected close to $\theta_3 = 180°$, resulting in an approximate, or bent, **T**-shape break-up pattern. If this distribution was determined solely by Coulomb repulsion between the electrons, the third electron distribution should peak near an angle of $225°$. It also appears that again the third electron is pushed slightly away from the polarization axis, as in Figure 1(c). Figure 1(d) also indicates a **T**-shape break-up pattern. In this example, we fix e_1 and e_2 back-to-back at $90°$ and $270°$, respectively, and find that the third electron is predominantly in the direction perpendicular to this axis, although again we observe that the ejection along the polarization direction is significantly suppressed. This, along with the expected symmetry about the e_1-e_2 axis, results in a 4-lobe angular distribution for the third electron. Finally, we also observe small peaks in Figure 1c

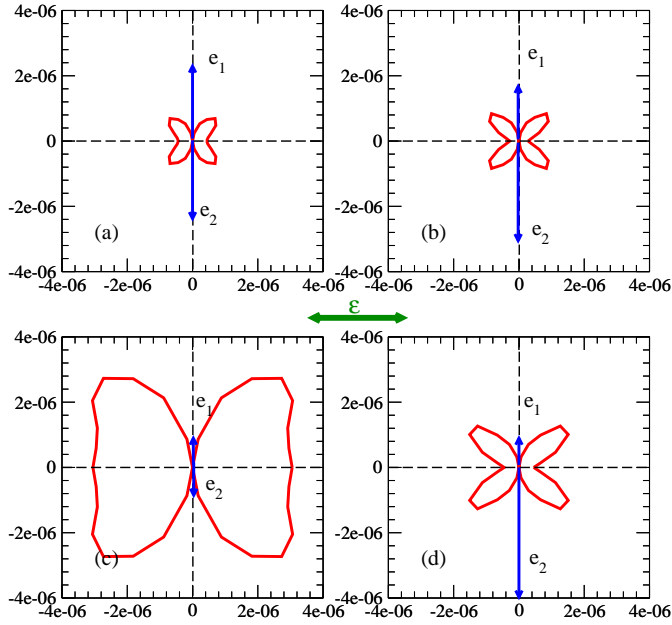FIG. 2: (Color online) Pentuple differential cross sections for triple photoionization of Li at a photon energy of 300 eV for $\theta_1 = 90°$, $\theta_2 = 270°$ and various energy sharings: (a): $E_1 = E_2 = E_3 = 33$ eV; (b): $E_1 = 20$, $E_2 = 40$, $E_3 = 40$ eV; (c): $E_1 = 10$, $E_2 = 10$, $E_3 = 80$ eV; (d): $E_1 = 10$, $E_2 = 45$, $E_3 = 45$ eV. All cross sections are in units of b/(sr^3 eV^2).

along directions where two electrons leave in the same direction. This is unphysical, and is due to the very slow convergence (with respect to the largest l value used) for these cross sections. However, the remaining (much larger) portion of the angular distribution is less sensitive to the l value used and is well converged by $l = 6$, as used in these calculations.

At a lower photon energy of 230 eV, we find similar angular distributions to those presented in Figure 1, except that we find that the **T**-shape break-up pattern is somewhat more favored. This is manifested by more pronounced side lobes in the 230 eV case for the same geometries shown in Figures 1(a) and (c). This is consistent with the earlier prediction [23] that the **T**-shape break-up completely dominates near threshold. At the larger electron energies found in triple photoionization by a 300 eV photon, the **T**-shape break-up competes with the "triangle" break-up geometry.

All the triple photoionization geometries so far discussed have been at equal energy sharing among the 3 outgoing electrons. In Figure 2 we turn to an example where unequal energy sharing electrons are ejected, for the back-to-back geometry where $\theta_1 = 90°$ and $\theta_2 = 270°$, again for a photon energy of 300 eV. In many double photoionization break-up geometries [4], the unequal energy sharing cases are often markedly different from the equal energy sharing case. This is chiefly due to the selection rule present in equal-energy sharing double photoionization which forbids back-to-back ejection [27]; unequal energy-sharing double photoionization distributions are usually strongly peaked at back-to-back geometries. In the triple photoionization case, no such strong selection rule exists for equal energy sharing, and we find that the unequal energy sharing cases are somewhat similar to the equal energy sharing case. We do find that, in general, the magnitude of the cross section is larger when the electrons do not have equal energy. For example, in Figure 2(c), where $E_1 = E_2 = 10$ eV and $E_3 = 80$ eV we find that the magnitude of the angular distribution of the third electron is almost three times larger than the equal energy sharing case (shown in Figure 2(a)). This is consistent with a photofragmentation picture where the photo-electron (most likely a $1s$ electron so that the nucleus can absorb the recoil momentum) is swiftly removed, and the remaining two electrons are ejected in a double shake-off event. Of course, one expects that at these energies, a knock-out mechanism has also some role to play in the triple photoionization process.

In Figure 3 we turn to a more general picture of the triple photoionization process, characterized by examining the angular distributions as a function of the *relative* angles between the three outgoing electrons, i.e. $\theta_{12}(= \theta_2 - \theta_1)$ and $\theta_{23}(= \theta_3 - \theta_2)$, again in the coplanar geometry, at equal energy sharing, and at a photon energy of 300 eV. This provides a quantity which is more comparable to the quasi-classical break-up predictions near threshold [23]. However such a comparison is again complicated by the choice of fixed electrons with respect to the polarization direction, which as demonstrated earlier, has a significant influence on the triple photoionization angular distributions (we
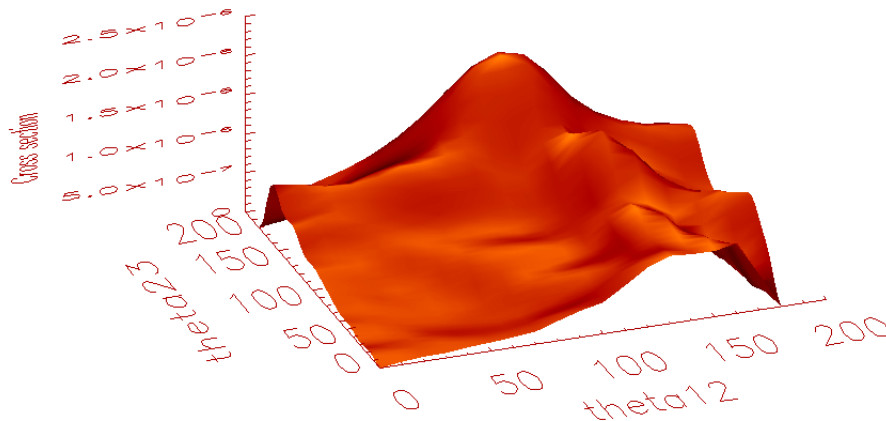
FIG. 3: (Color online) Pentuple differential cross sections for triple photoionization of Li at a photon energy of 300 eV, with equal energy sharing between all electrons, with fixed $\theta_1 = 90°$ and as a function of the relative angles θ_{12} and θ_{23} between the remaining two electrons. The cross section (z) axis has a maximum value of 2.5×10^{-6} b/(sr^3 eV^2).

remark here that the polarization axis does not enter into the quasi-classical calculations [23], so that *only* relative angle distributions may be computed). We choose in Figure 3 to fix the ejection direction of one electron at 90° (relative to the polarization direction), and plot the angular distributions as a function of θ_{12} and θ_{23}.

The most prominent feature of the distribution presented in Figure 3 is a large peak near $\theta_{12} = 90°$ and $\theta_{23} = 180°$. This corresponds to the first electron ejected along 90°, the second electron ejected along 180°, and the third electron ejected along 0°, i.e. a **T**-shape break-up. We thus confirm that an important break-up pattern for Li triple photoionization is a **T**-shape. The peak observed in Figure 3 is not quite at $\theta_{12} = 90°$, but is shifted to a slightly lower relative angle, reflecting again that that angular distribution is pushed away from the polarization axis, as found previously.

It is evident from the complex angular distribution of Figure 3 that there are more competing break-up channels which contribute to the triple photoionization. For example, we observe a prominent peak at $\theta_{12} \sim 120°$ and $\theta_{23} \sim 120°$, the angles that constitute the "triangle" break-up pattern. We also note that the distribution in Figure 3 is not symmetric about the $\theta_{12} = \theta_{23}$ axis; this is due to the initial choice to fix one electron at $\theta_1 = 90°$ with respect to the polarization axis.

In conclusion, we have presented the first *ab-initio* calculations of the angular distributions following complete break-up of Li by absorption of a single photon. Computation of these angular distributions poses many numerical and computational challenges due to the slow convergence with respect to the number of coupled channels and the inherently small cross sections. We find that the resulting electron angular distributions are complex, with several competing break-up channels evident. At photon energies near the peak of the total triple ionization cross section, the **T**-shape break-up pattern is dominant, but other break-up geometries also contribute. It is hoped that future experiments using synchrotron radiation, coupled with state-of-the-art multiple electron detection techniques, will provide an experimental check on the distributions presented here. However, the very small magnitude of the three-electron angular distributions poses a great challenge to experimental detection efficiencies.

[1] *Many-Body Atomic Physics*, eds. J. J. Boyle and M. S. Pindzola, (Cambridge Press, 1998).
[2] A. S. Kheifets and I. Bray, J. Phys. B **31**, L447 (1998).
[3] L. Malegat, P. Selles, and A. K. Kazansky, Phys. Rev. Lett. **85**, 4450 (2000).
[4] J. Colgan, M. S. Pindzola, and F. Robicheaux, J. Phys. B **34**, L457 (2001).
[5] T. N. Rescigno *et al*, Science **286**, 2474 (1999).
[6] J. Röder *et al*, Phys. Rev. Lett. **79**, 1666 (1997).
[7] T. Weber *et al*, Nature (London) **431**, 437 (2004).
[8] M. Gisselbrecht *et al*, Phys. Rev. Lett. **96**, 153002 (2006).
[9] W. Vanroose *et al*, Science **310**, 1787 (2005).
[10] T. J. Reddish *et al*, Phys. Rev. Lett. **100**, 193001 (2008).
[11] J. Colgan *et al*, Phys. Rev. Lett. **101**, 233201 (2008).
[12] M. Dürr *et al*, Phys. Rev. Lett. **98**, 193201 (2007).
[13] X. Ren, A. Dorn, and J. Ullrich, Phys. Rev. Lett. **101**, 093201 (2008).
[14] S. P. Cao *et al*, Phys. Rev. A **77**, 062703 (2008).
[15] M. S. Pindzola, F. Robicheaux, and J. Colgan, J. Phys. B **41**, 235202 (2008).
[16] Y.Hikosaka *et al*, Phys. Rev. Lett. **107**, 113005 (2011).
[17] A. I. Mikhailov, A. V. Nefiodov, and G. Plunien, Phys. Rev. Lett. **375**, 823 (2011).
[18] R. Wehlitz *et al*, Phys. Rev. Lett. **81**, 1813 (1998).
[19] T. Pattard and J. Burgdorfer, Phys. Rev. A **63**, 020701 (2001).
[20] A. W. Malcherek and J. S. Briggs, J. Phys. B **30**, 4419 (1997).
[21] A. W. Malcherek, J. M. Rost, and J. S. Briggs, Phys. Rev. A **55**, R3979 (1997).
[22] A. Emmanouilidou and J. M. Rost, J. Phys. B **39**, 4037 (2006).
[23] A. Emmanouilidou, P. Wang, and J. M. Rost, Phys. Rev. Lett. **100**, 063002 (2008).
[24] J. Colgan, M. S. Pindzola, and F. Robicheaux, Phys. Rev. Lett. **93**, 053201 (2004).
[25] J. Colgan, M. S. Pindzola, and F. Robicheaux, Phys. Rev. A **72**, 022727 (2005).
[26] J. Colgan and M. S. Pindzola, J. Phys. B **39**, 1879 (2006).
[27] F. Maulbetsch and J. S. Briggs, J. Phys. B **28**, 551 (1995).